

ONLINE FIRST

Hippocampal Interneurons in Bipolar Disorder

Christine Konradi, PhD; Eric I. Zimmerman, BS; C. Kevin Yang, BS; Kathryn M. Lohmann, BS; Paul Gresch, PhD; Harry Pantazopoulos, ALM; Sabina Berretta, MD; Stephan Heckers, MD

Context: Postmortem studies have reported decreased density and decreased gene expression of hippocampal interneurons in bipolar disorder, but neuroimaging studies of hippocampal volume and function have been inconclusive.

Objective: To assess hippocampal volume, neuron number, and interneurons in the same specimens of subjects with bipolar disorder and healthy control subjects.

Design: Whole human hippocampi of 14 subjects with bipolar disorder and 18 healthy control subjects were cut at 2.5-mm intervals and sections from each tissue block were either Nissl-stained or stained with antibodies against somatostatin or parvalbumin. Messenger RNA was extracted from fixed tissue and real-time quantitative polymerase chain reaction was performed.

Setting: Basic research laboratories at Vanderbilt University and McLean Hospital.

Samples: Brain specimens from the Harvard Brain Tissue Resource Center at McLean Hospital.

Main Outcome Measures: Volume of pyramidal and nonpyramidal cell layers, overall neuron number and size, number of somatostatin- and parvalbumin-positive interneurons, and messenger RNA levels of somatostatin, parvalbumin, and glutamic acid decarboxylase 1.

Results: The 2 groups did not differ in the total number of hippocampal neurons, but the bipolar disorder group showed reduced volume of the nonpyramidal cell layers, reduced somal volume in cornu ammonis sector 2/3, reduced number of somatostatin- and parvalbumin-positive neurons, and reduced messenger RNA levels for somatostatin, parvalbumin, and glutamic acid decarboxylase 1.

Conclusion: Our results indicate a specific alteration of hippocampal interneurons in bipolar disorder, likely resulting in hippocampal dysfunction.

Arch Gen Psychiatry. 2011;68(4):340-350.

Published online December 6, 2010.

doi:10.1001/archgenpsychiatry.2010.175

Author Affiliations:

Departments of Pharmacology (Drs Konradi and Gresch) and Psychiatry (Messrs Zimmerman and Yang, Ms Lohmann, and Dr Heckers), Vanderbilt University, Nashville, Tennessee; and Translational Neuroscience Laboratory, McLean Hospital (Mr Pantazopoulos and Dr Berretta), Belmont, and Department of Psychiatry, Harvard Medical School, Boston (Dr Berretta), Massachusetts.

BIPOLAR DISORDER AFFECTS about 2.6% of the US population¹ and is one of the leading causes of disability.² Despite its health impact, bipolar disorder is relatively understudied. Publications indexed in PubMed since 1980 with the term *schizophrenia* outweigh those with the term *bipolar disorder* by 8:1. This bias can be traced back to Emil Kraepelin's strong hypothesis that schizophrenia is a structural brain disorder, whereas bipolar disorder has no neural substrate.³

Genetic, neuroimaging, and postmortem studies are now challenging the Kraepelin dichotomy.⁴ Abnormalities of the limbic system are particularly compelling as neural substrates for the main features of bipolar disorder, such as depression, mania, psychosis, and cognitive deficits.⁵⁻⁷ However, the emerging literature on the hippocampus in bipolar dis-

order has been inconclusive. Neuroimaging studies have reported increases, decreases, or no changes of hippocampal volume in bipolar disorder.⁶⁻¹¹ Neuropsychological studies have demonstrated significant impairment of declarative memory in bipolar disorder,^{12,13} but this deficit has not been linked consistently to abnormalities of the hippocampus.^{7,14,15}

In contrast, postmortem studies have provided compelling evidence for abnormalities of the hippocampus in bipolar disorder. The initial finding of decreased nonpyramidal neuron density¹⁶ was confirmed and extended by an in situ hybridization study that revealed decreased expression of glutamic acid decarboxylase 1 (GAD1) messenger RNA (mRNA), coding for the enzyme that synthesizes γ -aminobutyric acid.¹⁷ Furthermore, the expression of mRNA coding for proteins expressed in subsets of hippocampal neurons was decreased in bipolar disorder.^{18,19} In concor-

dance, abnormalities of gene networks can be linked to distinct mechanisms of interneuron dysfunction in schizophrenia and bipolar disorder.²⁰⁻²² Taken together, the evidence for GABAergic dysfunction in bipolar disorder is compelling,^{23,24} though the structural correlates are still elusive.

In each of the 4 cornu ammonis sectors (CA1-4) of the hippocampus, GABAergic interneurons are interspersed with a much larger number of glutamatergic principal neurons. The ratio of glutamatergic to GABAergic neurons in the human hippocampus is in excess of 10:1,^{16,25} but a single interneuron provides inhibition through 1000 to 2000 synapses with principal neurons.^{26,27} Interneurons of the human hippocampus are crucial for the tonic and phasic inhibition of neighboring neurons, giving rise to characteristic electrical rhythms that are essential for cognitive processing.²⁸⁻³⁰

Herein, we used an unbiased stereological approach to determine overall neuron number and neuron size in whole hippocampal specimens. Furthermore, we measured the volume of pyramidal and nonpyramidal cell layers and we counted specific populations of GABAergic interneurons.

Hippocampal GABAergic neurons are classified based on the expression of calcium-binding proteins, such as parvalbumin, calbindin, and calretinin, and neuromodulators, such as somatostatin, neuropeptide Y, vasoactive intestinal peptide, and nitric oxide synthase.^{26,31} These "markers" identify subtypes of hippocampal interneurons with distinct morphological, physiological, and molecular properties.²⁷ We used whole hippocampal specimens to estimate the number of interneurons expressing somatostatin and parvalbumin. Somatostatin-releasing neurons make up 30% to 50% of all hippocampal interneurons.³² They control the efficacy and plasticity of excitatory inputs to principal neurons²⁶ and can modulate seizure activity.³³ Neurons expressing the calcium-binding protein parvalbumin play a key role in the generation of gamma oscillations,³⁴ which are abnormal in patients with cognitive impairments and psychiatric disorders.³⁵

We show herein that, in the context of normal total hippocampal neuron number, the number of somatostatin-positive and parvalbumin-positive hippocampal interneurons was markedly reduced in bipolar disorder. This finding was validated by the study of mRNA expression, using a novel real-time quantitative polymerase chain reaction (PCR) approach for fixed human brain tissue. Furthermore, the volume of the nonpyramidal cell layer was reduced, as was the cell body volume in sector CA2/3.

METHODS

SAMPLE

Brains were collected at the Harvard Brain Tissue Resource Center (McLean Hospital, Belmont, Massachusetts). The Harvard Brain Tissue Resource Center is funded by the National Institutes of Health and follows all regulations implemented by the Office for Human Research Protections.

For all the subjects included in this study, 2 psychiatrists established *DSM-IV* diagnoses based on the review of a ques-

tionnaire filled out by legal next of kin and a review of all available medical records. Control cases had sufficient information from next of kin and medical records to rule out major medical, neurologic, and psychiatric conditions. All brains underwent a neuropathological examination and cases with histopathological abnormalities were excluded from this study.

Two diagnostic groups, comprising 18 normal control subjects and 14 subjects with bipolar disorder, were matched for sex, age, postmortem interval (PMI), and hemisphere (**Table**). The sample included 14 matched pairs, which were chosen for the real-time quantitative PCR (QPCR) experiments (**Table**). Samples of the present study were newly collected and did not overlap with samples used in a previous study.¹⁷

TISSUE COLLECTION AND PROCESSING

The entire hippocampus was dissected from 1 hemisphere of each case. Tissue was immersion-fixed in paraformaldehyde, 4.0% (0.1M phosphate-buffered saline, pH 7.4), at 4.0°C for 3 weeks. Hippocampi were placed in cryoprotectant (0.1M phosphate-buffered saline, pH 7.4/sodium azide, 0.1%/ethylene glycol, 30.0%/glycerol, 30.0%), immersed in agar, and cut into 2.5-mm-thick coronal slabs using an antithetic tissue slicer. Sections were cut from the topmost portion of each slab using a sliding microtome (American Optical Company, Buffalo, New York), with a thickness of 100 μ m for Nissl stain or 50 μ m for immunocytochemical analysis. Sections were mounted on gelatin-coated glass slides and stained with cresyl violet, 0.1% (Nissl stain), or used for immunocytochemical analysis.

IMMUNOCYTOCHEMICAL ANALYSIS

The immunocytochemical procedure was performed as described previously.³⁶ For both immunocytochemical experiments, all sections were processed simultaneously to avoid procedural differences. Each staining dish contained sections from subjects with bipolar disorder and normal control subjects and all dishes were treated for the same duration (see the eAppendix for details of the procedure, <http://www.archgenpsychiatry.com>).

The somatostatin antibody was diluted 1:500 (monoclonal rat antisynthetic cyclic somatostatin peptide corresponding to amino acids 1-14, catalog No. MAB354; Millipore, Billerica, Massachusetts); the parvalbumin antibody was diluted 1:10 000 (monoclonal mouse antifrog muscle parvalbumin, clone PARV-19, catalog No. P3088; Sigma-Aldrich, St Louis, Missouri). Secondary antibodies were biotinylated goat antirat IgG for somatostatin and goat antimouse IgG for parvalbumin (Vector Laboratories, Burlingame, California). Secondary antibodies were diluted 1:500.

MORPHOMETRIC ANALYSIS

All cases were coded and data collection was completed without knowledge of diagnostic group. Morphometric analysis was performed using a Zeiss Axioskop 2 Plus microscope (Carl Zeiss, Oberkochen, Germany) equipped with a LEP MAC 5000 automated stage (Ludl Electronic Products, Hawthorne, New York). The microscope was interfaced with the Stereo Investigator stereological software (version 6.55; Microbrightfield, Colchester, Vermont) via an Optronics DEI-750 video camera (Optronics, Goleta, California). For the analysis of total neuron number and somal volume, we identified 1 pyramidal cell layer in 3 sectors (CA1, CA2/3, and CA4) and 2 nonpyramidal cell layers in sectors CA1 and CA2/3 (**Figure 1**, see eAppendix for details). For the analysis of somatostatin- and parvalbumin-positive neurons, we delineated 3 hippocampal sectors

Table. Demographics of All Study Subjects^a

Group	Patient No. ^{b/} Sex/Age, y	Hemisphere	PMI, h	Cause of Death	DSM-IV Diagnosis	Age at Onset, y	Duration of Illness, y	Family History	Psychotropic Medication
BPD	1/M/18	R	17.9	Motor vehicle accident	NA	17	1	NA	Bupropion hydrochloride
BPD	2/F/23	L	24.2	Suicide	BPD-I + P	16	7	Affective psychosis	Risperidone
BPD	3/M/38	L	22	Suicide (CO poisoning)	BPD-I	17	21	Psychosis	Lorazepam
BPD	4/F/40	R	21.9	Sepsis	BPD-I + P	22	18	Affective psychosis	
BPD	5/M/40	L	30.8	Suicide (hanging)	BPD-I + P	17	23	Mood disorder	Buspirone hydrochloride, ziprasidone hydrochloride
BPD	6/F/47	L	16.3	Major systems failure	BPD-I + P	18	29	Psychosis	Divalproex sodium
BPD	7/F/51	L	35.1	Ischemic heart disease	BPD-I + P	33	18	None	Clozapine, venlafaxine hydrochloride
BPD	8/F/52	L	17.2	Liver failure	BPD-I + P	26	26	Affective psychosis	Lithium
BPD	9/F/62	L	13.4	Congestive heart failure	BPD-I	NA	NA	NA	
BPD	10/M/70	L	17.3	Renal failure	BPD-I + P	27	43	Affective psychosis	Lithium
BPD	11/F/77	R	33.3	Pneumonia	BPD-I + P	NA	NA	NA	Olanzapine, clomipramine hydrochloride
BPD	12/F/78	R	24.8	Dehydration	BPD-I + P	28	50	Mood disorder	Lithium
BPD	13/F/79	L	22.6	Ovarian cancer	BPD-I + P	28	51	Affective psychosis	Trazodone, carbamazepine, gabapentin
BPD	14/M/83	R	32.9	Congestive heart failure	BPD-I + P	29	54	Affective psychosis	Olanzapine, divalproex sodium, mirtazapine
Control	1/M/22	R	21.5	Myocardial infarct					
Control	2/F/36	R	18.1	Cardiac arrest					
Control	3/M/35	L	25.7	Myocardial infarct					
Control	4/F/42	L	20.3	Myocardial infarct					
Control	5/M/41	R	27.2	Cardiac arrest					
Control	6/F/51	R	23.1	Cardiac arrest					
Control	7/F/55	R	27.5	Cardiopulmonary arrest					
Control	8/F/58	L	21.1	Myocardial infarct					
Control	9/F/60	L	12.5	Breast cancer					
Control	10/M/68	L	18.4	Heart failure					
Control	11/F/68	R	23.9	Cardiopulmonary arrest					
Control	12/F/74	L	23	Pneumonia					
Control	13/F/81	R	17.4	Colon cancer					
Control	14/M/77	L	24.6	Cardiac arrest					
Control	15/M/52	L	13.1	Heart disease					
Control	16/F/60	R	17.8	Cardiac dysrhythmia					
Control	17/M/60	L	30.3	Cardiac arrest					
Control	18/F/86	L	6.9	Cardiac arrest					

Group	No. of Subjects	Age, y, Mean (SD)	Sex (F/M)	Hemisphere (L/R)	PMI, h, Mean (SD)
BPD	14	54.1 (21.2)	9/5	9/5	23.5 (7.0)
Control 1	14	54.9 (17.8)	9/5	7/7	21.7 (4.2)
Control 2	18	57.0 (17.3)	11/7	10/8	20.7 (5.9)

Abbreviations: BPD, bipolar disorder; BPD-I, BPD type I; CO, carbon monoxide; Control 1, control subjects included in the QPCR experiment; Control 2, all subjects in the control group; NA, not available; +P, with psychosis; PMI, postmortem interval; QPCR, quantitative polymerase chain reaction.

^aSubjects with BPD were diagnosed according to *DSM-IV* criteria. For 13 subjects, sufficient information was available to subtype (1) BPD type I or II and (2) BPD + P or BPD without psychosis. For 11 subjects, information was available to diagnose a family history of nonpsychotic mood disorder (n=2), affective psychosis (n=6), psychosis (n=2), or no psychiatric disorder (n=1).

^bSubjects 1 to 14 in each group were matched pairwise for age and sex. These pairs were used for the QPCR experiment.

(CA1, CA2/3, and CA4) without further separation into layers (**Figure 2**, see eAppendix for details).

VOLUME AND TOTAL NEURON NUMBER ESTIMATES

Uniformly random sampling of CA neurons was conducted in the pyramidal cell layer throughout the entire hippocampal formation. Sections were sampled at a fixed interval of 2.5 mm with a random starting point in the coronal plane (average of 17 sections per hippocampus). Volume estimates of layers in

the CA sectors were calculated from the product of known intervals between sections and contour measurements. Weighted means for section thicknesses were determined at every sampling site by differential focusing using a ×100 oil-immersion objective (Plan-Apochromat, NA 1.40; Carl Zeiss). The vertical movement of the stage was determined by a microcator (Heidenhain, Traunreut, Germany).

The optical fractionator method was used to obtain an unbiased estimate of total neuron number in each of the CA sectors. The optical fractionator approach is independent of volume measurements and is unaffected by tissue shrinkage in the

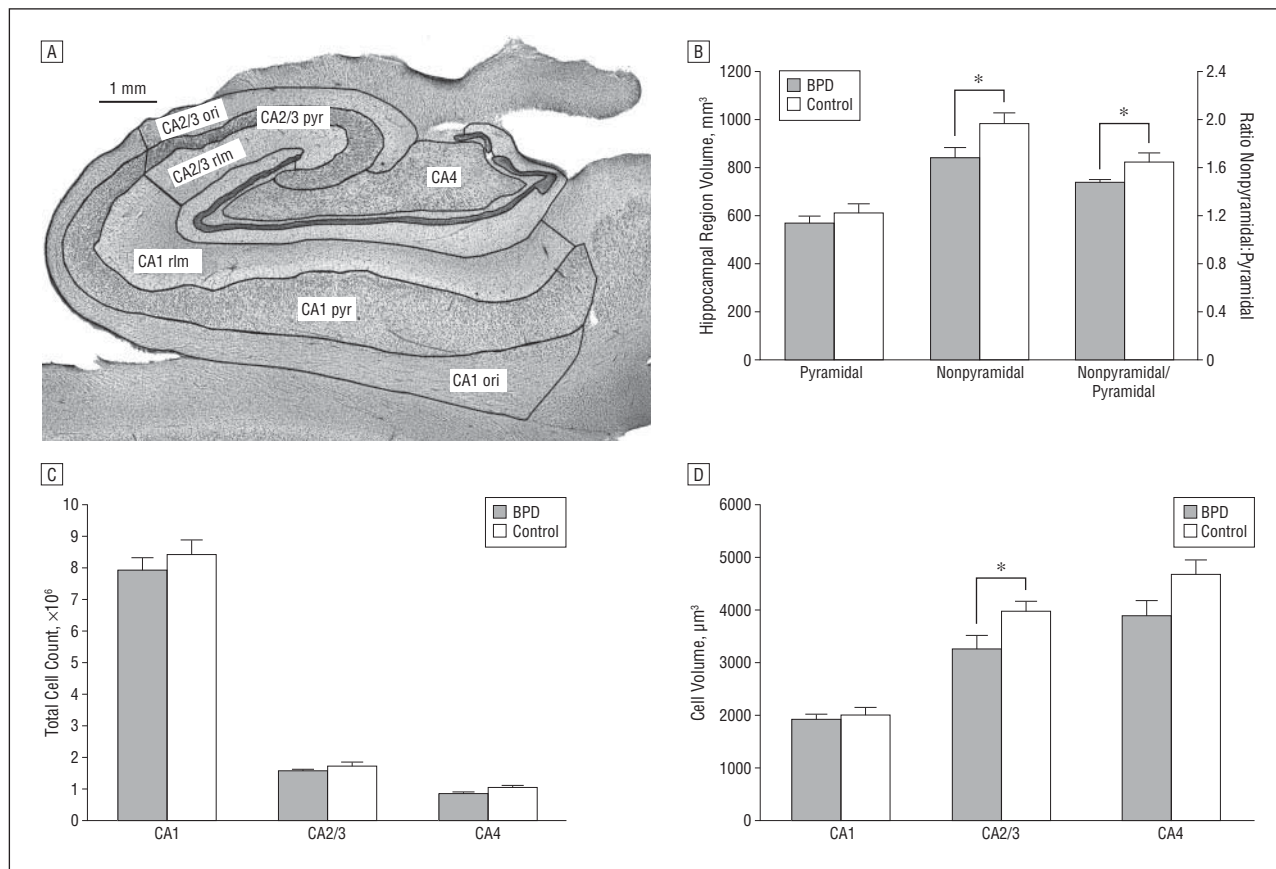


Figure 1. Hippocampal anatomy and cellular organization. A, Coronal section through the body of the hippocampus. The cornu ammonis 1 (CA1) and CA2/3 sectors have 3 layers: stratum oriens (ori), stratum pyramidale (pyr), and stratum radiatum/lacunosum/moleculare (rim). The CA4 sector has stratum pyramidale only. B, Ratio of pyramidal and nonpyramidal cell layer volumes in control subjects and subjects with bipolar disorder (BPD). Nonpyramidal cell layers are reduced in bipolar disorder. C, Similar cell numbers in the pyramidal cell layer in the CA1 to CA4 sectors of control subjects and subjects with BPD. D, Average neuronal cell volume in the CA1 to CA4 sectors of control subjects and subjects with BPD. There is a reduction in cell volume in CA2/3. Mean (SD) values are presented in parts B-D. * $P \leq .05$.

z-axis.^{37,38} Neurons were counted within a 3-dimensional dissector box ($50 \times 50 \times 10 \mu\text{m}$). Dissector counting frames were positioned in a systematically random fashion in each CA sector ($1200 \times 1200 \mu\text{m}$ for CA1 and $600 \times 600 \mu\text{m}$ for CA2/3 and CA4). Neurons were counted only when their associated nucleoli were in focus within the dissector box and not touching the left or bottom side of the dissector box.³⁹ To avoid the issues of lost caps and other cutting artifacts, a 2- μm guard zone was applied to the top and bottom of each section.³⁹ This stereological sampling protocol resulted in the following average cell count (Q), counting sites (F), and average estimated volume coefficients of errors (CE): CA1 = 284/131/0.06 (Q/F/CE); CA2/3 = 242/104/0.07 (Q/F/CE); and CA4 = 144/116/0.09 (Q/F/CE).

The estimate of total neuron number per CA sector was calculated as the product of the number of neurons counted within the dissector box (ΣQ) and the reciprocal of the fraction of the CA sector sampled.⁴⁰ The reciprocal fraction is the product of the fraction of the sections sampled, the fraction of the area of the sections sampled, and the fraction of the section thickness sampled. This last fraction is given as the ratio of dissector box height to number-weighted mean section thickness, which is calculated from the local section thickness and local neuron count in the i th counting frame. This estimation allows thickness calculations to be unbiased even if homogeneous, nonuniform deformation in the z-axis occurs^{37,38} (average section thickness in our samples: CA1, 20.45 μm ; CA2/3, 19.69 μm ; and CA4, 19.25 μm).

SOMAL VOLUME ESTIMATES

The nucleator method^{41,42} was used to estimate somal volume of neurons in each of the CA sectors. The nucleator probe superimposed 4 isotropic rays emanating from the nucleolus of each sampled neuron. Estimates of area and volume were calculated from the recorded distance between the nucleolus and cell wall for each ray. Neurons were sampled from sections at 7.5-mm intervals. The counting frame dimensions were $2500 \times 2500 \mu\text{m}$ for the CA1 sector and $1000 \times 1000 \mu\text{m}$ for the CA2/3 and CA4 sectors. This resulted in the following average cell count (Q), counting sites (F), and estimated volume coefficients of errors (CE) per sector: CA1 = 54.8/17.1/0.01 (Q/F/CE); CA2/3 = 57.7/14.2/0.01 (Q/F/CE); and CA4 = 41.8/15.4/0.02 (Q/F/CE).

TOTAL IMMUNOPosITIVE NEURON ESTIMATES

The somatostatin- and parvalbumin-positive neurons were assessed in sections of 5-mm intervals. First, volume estimates of the 3 CA sectors were calculated from the product of known intervals between sections and contour measurements. Second, using the automated stage of the microscope, each section was systematically scanned through the full x-, y-, and z-axes using a $\times 40$ objective to count each parvalbumin- and somatostatin-labeled element with a cell body and at least 1 process clearly identifiable within each of the 3 CA sectors

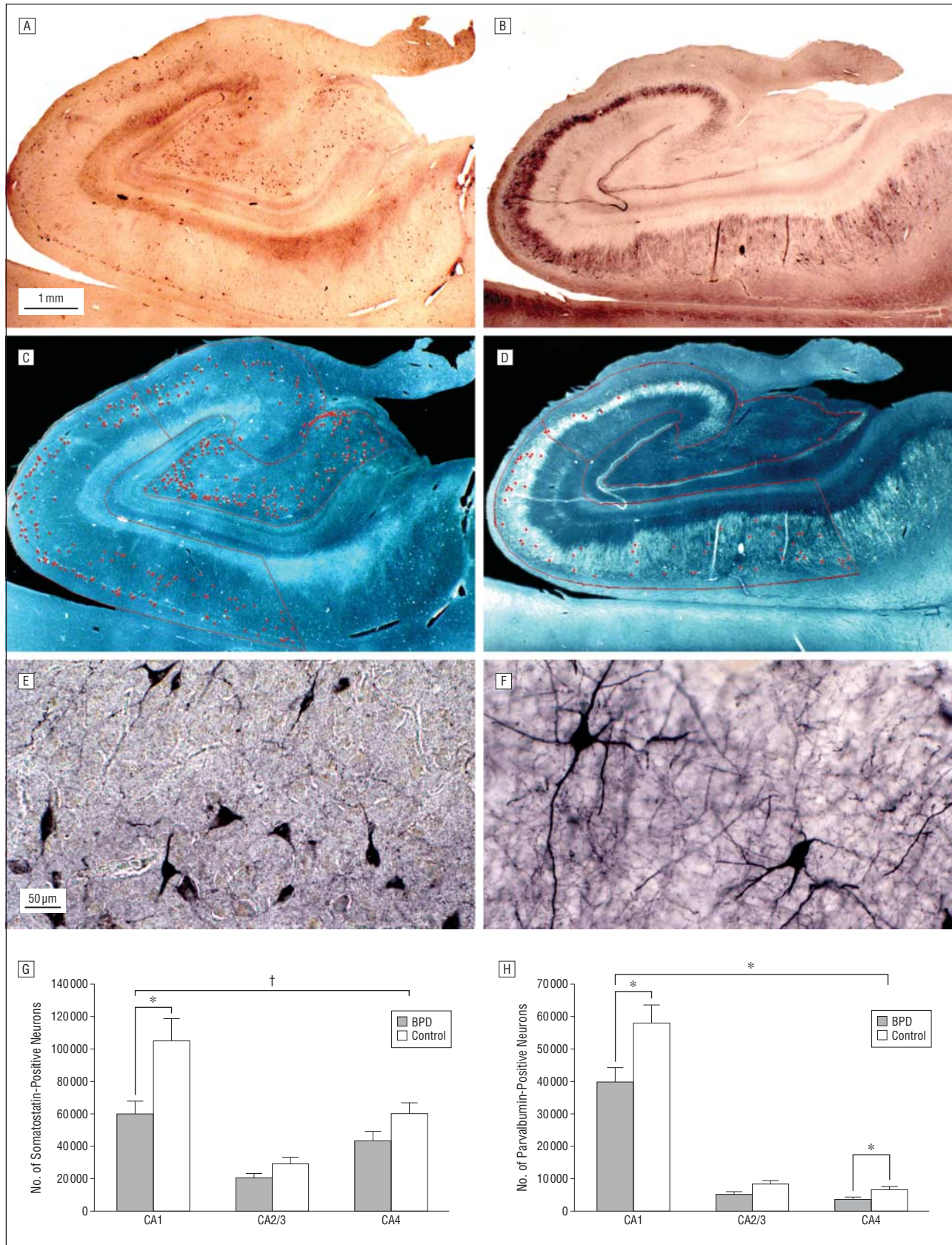


Figure 2. Somatostatin-positive and parvalbumin-positive hippocampal interneurons. An overall reduction of somatostatin-positive (A, C, E, and G) and parvalbumin-positive (B, D, F, and H) neurons was observed in all sectors of the hippocampus. Post hoc analysis revealed the sectors with the most significant changes. A and B, Representative control case showing immunohistochemical stain. C and D, Overlay of counted cells and hippocampal sectors onto stained tissue. E and F, Individually stained cells. G and H, Bar graphs and statistics of all 14 subjects with bipolar disorder (BPD) and 18 control subjects. Mean (SD) values are presented in parts G and H. * $P \leq .05$. † $P \leq .01$. Scale bar in part A applies to parts A-D. Scale bar in part E applies to parts E and F.

(Figure 2). The average regional coefficients of error were 0.02 (CA1 and CA4) and 0.03 (CA2/3). Third, the total number of somatostatin- and parvalbumin-positive neurons was calculated as total number of cells counted/50 $\mu\text{m} \times 5000 \mu\text{m}$.

REAL-TIME QPCR

Three hippocampal sectors (CA1, CA2/3, and CA4) were dissected from a 2.5-mm slab of fixed, frozen tissue, collected from the middle body of the hippocampus, and RNA was extracted using the Recoverall Total Nucleic Acid Isolation kit (Applied Biosystems, Foster City, California). Cornu ammonis borders were determined on an adjacent cresyl violet-stained slice. The tissue was digested with protease, RNA isolated onto a glass filter, washed, and eluted with water. Samples were vacuum dried and resuspended in a volume of 20 μL of water. RNA quantity was measured using the NanoDrop 1000A Spectrophotometer (Thermo Fisher Scientific, Wilmington, Delaware), with A260:A280 ratios ranging from 1.8 to 2.1.

One microgram of RNA was reverse transcribed into complementary DNA (cDNA) using the High-Capacity cDNA Reverse Transcription Kit (Applied Biosystems). Reverse transcription was performed in an Eppendorf Mastercycler (Eppendorf, Hamburg, Germany) for 10 minutes at 25°C, 120 minutes at 37°C, and 5 seconds at 85°C. The TaqMan PreAmp Master Mix Kit (Applied Biosystems) was used to increase the quantity of specific cDNA targets for QPCR analysis. For the preamplification reaction, the primers and probes of 5 TaqMan assays (*SST*, *PVALB*, *GAD1*, *ACTB*, and *FLNA*) were pooled together, with 1 \times TRIS-EDTA buffer. The preamplification reaction was performed in 50- μL reactions containing 25 μL of TaqMan PreAmp Master Mix, 12.5 μL of the pooled assay mix, 10 μL of cDNA sample, and 2.5 μL of nuclease-free water. Cycling conditions were 10 minutes at 95°C, 14 cycles of 15 seconds at 95°C, and 4 minutes at 60°C using an Eppendorf Mastercycler.

The preamplified products were diluted 1:20 using 1 \times TRIS-EDTA buffer. The gene expression reaction was performed in 20- μL reactions containing 10 μL of TaqMan Gene Expression Master Mix, 5 μL of diluted preamplified product, and 1 μL of TaqMan gene expression assay and 4 μL of nuclease-free water (Applied Biosystems). A standard curve was generated using five 1:5 dilutions of pooled preamplified products. The logarithm of the dilution value was plotted against the cycle threshold value. Each dilution curve contained blanks to control for cross-contamination. Dilution curves and blanks were run in duplicate and samples were run in triplicate. The following thermal cycling specifications were performed on the Stratagene Mx3005P instrument (Stratagene, Agilent Technologies, Inc, Santa Clara, California): 2 minutes at 50°C, 10 minutes at 95°C, and 40 cycles each for 15 seconds at 95°C and 1 minute at 60°C (reading temperature). The Stratagene MxPro QPCR software used the cycle threshold data from the standards to quantify the cDNA for subject samples. Gene expression was normalized to β -actin and the actin binding protein filamin A, the latter of which has been shown to have equal expression levels in the hippocampus in subjects with bipolar disorder and controls.¹⁸ Within each experiment, 96 data points could be collected, with 12 data points used for standard curves and blanks. Thus, for each sector, 28 samples were examined in triplicate, and matched pairs of subjects with bipolar disorder and control subjects were used (Table).

EFFECT OF TREATMENT ON SOMATOSTATIN, PARVALBUMIN, AND GAD1 mRNA LEVELS

Male Sprague-Dawley rats (weighing 200-250 g at the start of treatment) were treated long-term with either lithium, val-

proic acid, clozapine, or haloperidol and hippocampi were subjected to gene expression analysis. The eTable shows treatment durations, subject numbers, route of administration, types of gene arrays used, and mRNA levels of somatostatin, parvalbumin, and GAD1.

STATISTICAL ANALYSIS

Histological data were analyzed for subjects used in the QPCR analysis ($n = 14$ per diagnostic group) and in the complete data set ($n = 14$ subjects with bipolar disorder, $n = 18$ controls) (Table). We did not observe any significant difference between these 2 analyses and are reporting herein the analysis of the complete data set. Hippocampal sectors were treated as repeated measures. To reduce the weight of outliers, all histological data were \log_2 -transformed for analysis. Initially, multivariate analysis of covariance was performed with "diagnosis" as the between-subject effect and "CA sector" as the within-subject effect. Covariates included sex, age, PMI, and hemisphere, as indicated in the "Results" section. In case of a significant diagnosis effect in the multivariate analysis of covariance model, we tested for group differences in individual CA sectors using the *t* test and Cohen *d* effect size calculation. Because of the 96-well limitation in QPCR experiments, samples had to be grouped into CA sectors and each CA sector was independently analyzed. The JMP program (version 7.02; SAS Institute Inc, Cary, North Carolina) was used for all analyses.

RESULTS

HIPPOCAMPAL VOLUME, CELL NUMBER, AND CELL VOLUME

We studied volume and cell number in systematically sampled coronal sections of whole hippocampal specimens. In each section, we differentiated up to 3 sectors (CA1, CA2/3, and CA4) and 3 layers (stratum oriens, stratum pyramidale, stratum radiatum/lacunosum/moleculare) (Figure 1A). While hippocampal volume is a biased estimate because of postmortem tissue shrinkage, the ratio of pyramidal to nonpyramidal cell layer volumes is not. We found similar volumes of the CA1:CA4 pyramidal cell layer in the 2 groups, but the volume of the CA1:CA3 nonpyramidal cell layers was significantly smaller in bipolar disorder (main effect of diagnosis: $F_{3,26} = 5.57$; $P \leq .03$ with age, sex, hemisphere, and PMI as covariates; Cohen $d = 0.84$) (Figure 1B).

The mean (SEM) total number of neurons in pyramidal layers CA1 to CA4 was 10 877 208 (386 524), with the largest number in CA1 (8 228 372 [303 270]) and significantly fewer numbers in CA 2/3 (1 665 760 [84 561]) and CA 4 (983 077 [43 972]) (main effect of sector: $F_{2,25} = 7.7$; $P \leq .002$ with age, sex, hemisphere, and PMI as covariates). This pattern did not differ significantly between the 2 groups (main effect of diagnosis: $F_{1,26} = 0.8$; $P \leq .37$ with age, sex, hemisphere, and PMI as covariates) (Figure 1C).

Average cell volume was similar across the 3 sectors (main effect of sector: $F_{2,25} = 1.4$; $P \leq .27$ with diagnosis, age, sex, hemisphere, and PMI as covariates) and across the 2 groups (main effect of diagnosis: $F_{1,26} = 2.8$; $P \leq .10$ with age, sex, hemisphere, and PMI as covariates). However, a significant interaction was observed between di-

agnosis and sector ($F_{2,25}=3.7$; $P \leq .04$ with age, sex, hemisphere, and PMI as covariates) because of the significantly smaller cell volume of CA2/3 neurons in bipolar disorder ($t_{1,30}=-2.34$; $P \leq .03$; Cohen $d=0.82$) (Figure 1D).

SOMATOSTATIN- AND PARVALBUMIN-POSITIVE INTERNEURONS

We estimated the total number of somatostatin- and parvalbumin-positive hippocampal interneurons in sections adjacent to the Nissl-stained sections reviewed earlier. Somatostatin-positive neurons were small neurons with sparse labeling of the axon and dendritic tree and were found in pyramidal and nonpyramidal cell layers of sectors CA1 to CA4 (Figure 2A, C, and E). Parvalbumin-positive neurons were larger neurons with extensive labeling of both the axon and dendritic tree and were found almost exclusively in the pyramidal cell layer (Figure 2B, D, and F).

The total number of somatostatin-positive neurons was largest in CA1 and smallest in CA2/3. This pattern was similar in both groups, but the total number of somatostatin-positive neurons was significantly reduced in subjects with bipolar disorder ($F_{1,26}=8.7$; $P \leq .007$ with age, sex, hemisphere, and PMI as covariates) (Figure 2G). Sector CA1 ($t_{1,30}=-2.28$; $P \leq .03$; Cohen $d=0.82$) reached significance in a post hoc analysis.

The total number of parvalbumin-positive neurons was largest in CA1 and smallest in CA4. This pattern was similar in both groups, but the total number of parvalbumin-positive neurons was significantly reduced in subjects with bipolar disorder ($F_{1,24}=5.4$; $P \leq .03$ with age, sex, hemisphere, and PMI as covariates) (Figure 2H). Sectors CA1 ($t_{1,28}=-2.28$; $P \leq .03$; Cohen $d=0.83$) and CA4 ($t_{1,28}=-2.27$; $P \leq .03$; Cohen $d=0.84$) reached significance in a post hoc t test.

GENE EXPRESSION LEVELS OF HIPPOCAMPAL INTERNEURONS

We studied hippocampal mRNA expression levels of somatostatin, parvalbumin, and GAD1 in a subsample of the cases reviewed earlier (Table). Normalized mRNA expression levels of somatostatin were significantly lower in bipolar disorder (Figure 3). Differences in sectors CA1 ($t_{1,24}=-2.29$; $P \leq .03$; Cohen $d=0.90$), CA2/3 ($t_{1,24}=-2.5$; $P \leq .02$; Cohen $d=0.98$), and CA4 ($t_{1,24}=-2.1$; $P \leq .046$; Cohen $d=0.83$) reached significance. Normalized mRNA expression levels of parvalbumin were also significantly lower in bipolar disorder (Figure 3). Differences in sectors CA2/3 ($t_{1,24}=-2.38$; $P \leq .03$; Cohen $d=0.93$) and CA4 ($F_{1,24}=-2.94$; $P \leq .007$; Cohen $d=1.15$) reached significance. Finally, normalized GAD1 mRNA levels were significantly reduced in CA2/3 ($t_{1,24}=-2.2$; $P \leq .04$; Cohen $d=0.864$).

EFFECT OF TREATMENT

mRNA analysis of groups of rats treated with lithium carbonate, valproic acid, or antipsychotic drugs did not show any effect of treatment on levels of somatostatin, parvalbumin, or GAD1 (eTable).

This study, using unbiased cell counting, immunocytochemical analysis, and real-time QPCR in the same specimens, provides strong evidence for a marked reduction of somatostatin- and parvalbumin-positive interneurons in bipolar disorder. While the number of these 2 subtypes of hippocampal interneurons was significantly reduced, total neuron number and the volume of the pyramidal cell layer were not different from the healthy control group. This confirms and considerably extends previous studies of hippocampal interneurons in bipolar disorder.^{16,17}

Neuroimaging studies have reported conflicting results regarding hippocampal volume in bipolar disorder, in contrast to the overwhelming evidence for smaller hippocampal volume in schizophrenia⁴³ and depression.⁷ Several recent meta-analyses have now concluded that overall hippocampal volume is not abnormal in bipolar disorder.^{10,11,44,45} Our finding of significantly reduced nonpyramidal (but normal pyramidal) cell layer volume in bipolar disorder provides compelling evidence for a subtle volume difference of the hippocampus, beyond the resolution of current imaging studies. The major components of the nonpyramidal cell layers in the human hippocampus are axonal projections (primarily from neurons within the hippocampus) and a variety of interneurons, including their extensive dendritic arborization.^{26,27,46} It is unlikely that the axons of projection neurons are markedly abnormal in bipolar disorder, since total cell number and regional volume of the pyramidal cell layer were normal. However, the number of immunopositive interneurons was reduced, which likely reduces their rich dendritic arborization, primarily in the stratum radiatum/lacunosum/moleculare. Therefore, we interpret the pattern of volume change observed in the subjects with bipolar disorder as further support for hippocampal interneuron pathology in bipolar disorder. New structural imaging protocols are now approaching the resolution necessary to identify the pyramidal and nonpyramidal cell layers in the CA sectors of the human hippocampus.⁴⁷⁻⁵⁰ Future neuroimaging studies should test for a layer-specific reduction of hippocampal volume in bipolar disorder.

Previous anatomical studies had demonstrated reduced density of hippocampal interneurons¹⁶ and reduced expression of GAD1 mRNA¹⁷ in bipolar disorder. However, it was not known whether this pattern was part and parcel of an overall reduced neuron number. It was also not clear which subtypes of hippocampal interneurons are affected in bipolar disorder. Our study clarifies the existing literature since it provides strong evidence that the reduced number of 2 functionally important hippocampal interneurons is not in the context of an overall loss of hippocampal neurons in bipolar disorder. This has implications for several types of hippocampal information processing in bipolar disorder, which we briefly outline herein.

Hippocampal interneurons modulate the activity of the principal (ie, glutamatergic) hippocampal neurons, resulting in an increased signal to noise ratio and synchronized

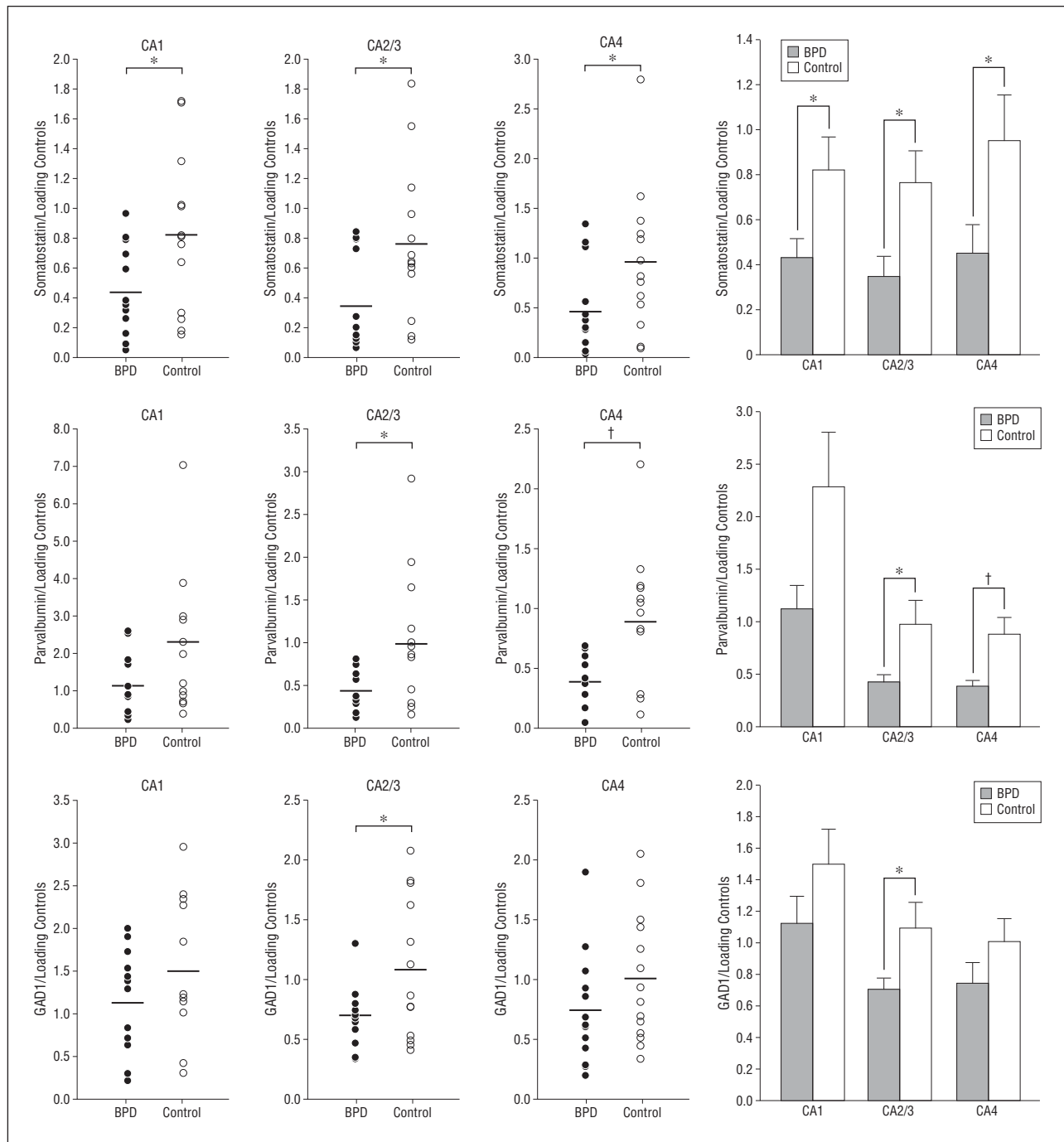


Figure 3. Real-time quantitative polymerase chain reaction analysis of somatostatin, parvalbumin, and glutamic acid decarboxylase 1 (GAD1) in the hippocampus. Real-time quantitative polymerase chain reaction showed a reduction of somatostatin messenger RNA (mRNA) levels in all cornu ammonis (CA) sectors. A reduction of parvalbumin mRNA was observed in sectors CA2/3 and CA4. The GAD1 mRNA levels were reduced in sector CA2/3. Distribution and bar graphs of 14 subjects with bipolar disorder (BPD) and 14 control subjects. All data were normalized to β -actin and filamin A, averaged. Mean (SD) values are presented. * $P \leq .05$. † $P \leq .01$.

network activity. Fast oscillations in the gamma range (30–100 Hz) provide an organized pattern for the temporal encoding of new information and the storage and recall of previously stored information.^{51–53} Parvalbumin-expressing interneurons are crucial for the generation of gamma oscillations.³⁴ A reduction of parvalbumin-positive neurons leads to a loss of perisomatic inhibition of pyramidal neurons, which in turn affects network synchronization and memory formation.^{34,35} Previous studies have provided com-

pellent evidence that several neuropsychiatric disorders, including schizophrenia, are characterized by disrupted gamma oscillation.^{54–56} Our findings provide compelling evidence that a similar pattern of dysfunction is also present in bipolar disorder.

Between 30% to 50% of all interneurons in the hippocampus contain the neuromodulator somatostatin.³² Somatostatin-positive interneurons ameliorate perturbations in glutamatergic neurotransmission, which has been

found to be abnormal in affective disorders.^{57,58} These neurons regulate the efficacy and plasticity of excitatory inputs to principal neurons²⁶ and play an important role in the control of seizure activity.³³ Our finding of reduced somatostatin-positive hippocampal interneurons suggests that hippocampal disinhibition is a feature of bipolar disorder and that interneurons are a potential site of action for anticonvulsants, a class of drugs with proven benefit in the treatment of bipolar disorder, particularly mania.⁵⁹

We can only speculate about the behavioral implication of reduced hippocampal interneuron number in bipolar disorder. On the one hand, reciprocal connections of the posterior hippocampus ensure that the constructive process of memory encoding and retrieval creates accurate representations of experience.^{60,61} On the other hand, projections to and from the anterior hippocampus regulate affective processes.⁶² It is likely that impairments in these hippocampal functions^{63,64} lead to poor functional outcomes in patients with bipolar disorder.^{13,65}

We did observe a significant decrease in the size of hippocampal neurons, most pronounced in sector CA2/3, in line with a similar report of decreased pyramidal cell size in CA1 in bipolar disorder.⁶⁶ The somal size of adult hippocampal neurons could be a distal read-out of neurodevelopmental abnormalities or a more proximal consequence of malfunction of trophic factors and synaptic remodeling during adulthood. Risk genes associated with psychotic disorders, including *DISC1* and neuregulin, have been associated with regulation of neuronal size.^{67,68} Somal size remains plastic during adulthood and the known change of hippocampal volume during lithium treatment^{69,70} could be mediated through changes in neuronal size. Concurrently, the normal decrease of somal size during adulthood could be accelerated in bipolar disorder, explaining the hippocampal volume reduction found in some adult bipolar disorder samples.⁷¹

Our study design does have limitations. First, the sample size is small, in large part because whole hippocampal specimens are difficult to obtain. However, the effect sizes of the total somatostatin- and parvalbumin-positive neuron number reduction were reassuringly large.

Second, it is not clear whether our findings in a severely ill group of subjects with psychotic bipolar disorder can be generalized to the larger group of subjects with bipolar disorder. The majority of patients in our study were diagnosed retrospectively with *DSM-IV-TR* bipolar disorder type I with psychotic features. The average age at onset was 23 years and average duration of illness was 28 years. For 8 of the 14 subjects with bipolar disorder, we could identify a first-degree relative with an affective or nonaffective psychotic disorder.

Third, the immunopositive neurons were not studied with the fractionator or dissector and the sampling regions differed between the Nissl and immunocytochemical stains. This is similar to previous studies^{36,72} and was because of the requirement to have consistent and reliable criteria for the demarcation of the reference volume and the objects to be sampled. Fourth, the total number estimates of the somatostatin- and parvalbumin-positive neuron number in the human hippocampus are affected by several confounding postmortem effects⁷³ and may be an underestimate.^{26,74} However, there is no rea-

son to assume that this potential bias is limited to the bipolar disorder group only. Finally, effects of treatment cannot be ruled out, though we examined mRNA levels of somatostatin, parvalbumin, and GAD1 in rat hippocampi and could not find any effect of drugs commonly prescribed in bipolar disorder.

Our study contributes to the evolving nosology of psychotic disorders. There is now compelling evidence for shared genetic mechanisms of both psychotic bipolar disorder and schizophrenia.^{4,75} Our results confirm and extend previous findings of hippocampal interneuron pathology in both affective and nonaffective psychosis.^{19,22} This will lead to novel models of disease mechanism beyond the Kraepelinian dichotomy.^{76,77}

In conclusion, we present strong evidence for significant abnormalities of hippocampal interneurons in bipolar disorder type I. These findings have major implications for models of information processing in bipolar disorder and provide a rationale for the efficacy of existing,⁷⁸ and the development of novel, pharmacological interventions of this major psychiatric disorder.

Submitted for Publication: June 18, 2010; final revision received September 30, 2010; accepted October 4, 2010.

Published Online: December 6, 2010. doi:10.1001/archgenpsychiatry.2010.175

Correspondence: Christine Konradi, PhD, Vanderbilt University, MRB 3, Room 8160A, 465 21st Ave S, Nashville, TN 37232-8548 (christine.konradi@vanderbilt.edu).

Author Contributions: Dr Konradi had full access to all of the data in the study and takes responsibility for the integrity of the data and the accuracy of the data analysis.

Financial Disclosure: None reported.

Funding/Support: This work was supported by National Institute of Mental Health grants MH67999 (Dr Heckers), MH74000 (Dr Konradi), and MH068855 (Francine M. Benes, MD, PhD, Harvard Brain Tissue Resource Center).

Disclaimer: The content is solely the responsibility of the authors and does not necessarily represent the official views of the funding institute or the National Institutes of Health.

Online-Only Material: The eAppendix and eTable are available at <http://www.archgenpsychiatry.com>.

REFERENCES

1. Kessler RC, Chiu WT, Demler O, Merikangas KR, Walters EE. Prevalence, severity, and comorbidity of 12-month *DSM-IV* disorders in the National Comorbidity Survey Replication [*Arch Gen Psychiatry*. 2005;62(7):709]. *Arch Gen Psychiatry*. 2005;62(6):617-627.
2. Lopez AD, Mathers CD, Ezzati M, Jamison DT, Murray CJL. *Global Burden of Disease and Risk Factors*. Washington, DC: World Bank and Oxford University Press; 2006.
3. Kraepelin E. *Psychiatrie. Ein Lehrbuch für Studierende und Ärzte. Achte, vollständig umgearbeitete Auflage. 3. Band. Klinische Psychiatrie. 2. Teil*. Leipzig, Germany: Verlag von Johann Ambrosius Barth; 1913.
4. Craddock N, Owen MJ. Rethinking psychosis: the disadvantages of a dichotomous classification now outweigh the advantages. *World Psychiatry*. 2007; 6(2):84-91.
5. Phillips ML. The neural basis of mood dysregulation in bipolar disorder. *Cogn Neuropsychiatry*. 2006;11(3):233-249.

6. Brambilla P, Hatch JP, Soares JC. Limbic changes identified by imaging in bipolar patients. *Curr Psychiatry Rep*. 2008;10(6):505-509.
7. Savitz J, Drevets WC. Bipolar and major depressive disorder: neuroimaging the developmental-degenerative divide. *Neurosci Biobehav Rev*. 2009;33(5):699-771.
8. Keener MT, Phillips ML. Neuroimaging in bipolar disorder: a critical review of current findings. *Curr Psychiatry Rep*. 2007;9(6):512-520.
9. Konarski JZ, McIntyre RS, Kennedy SH, Rafi-Tari S, Soczynska JK, Ketter TA. Volumetric neuroimaging investigations in mood disorders: bipolar disorder versus major depressive disorder. *Bipolar Disord*. 2008;10(1):1-37.
10. Bora E, Fornito A, Yücel M, Pantelis C. Voxelwise meta-analysis of gray matter abnormalities in bipolar disorder. *Biol Psychiatry*. 2010;67(11):1097-1105.
11. Ellison-Wright I, Bullmore E. Anatomy of bipolar disorder and schizophrenia: a meta-analysis. *Schizophr Res*. 2010;117(1):1-12.
12. Robinson LJ, Ferrier IN. Evolution of cognitive impairment in bipolar disorder: a systematic review of cross-sectional evidence. *Bipolar Disord*. 2006;8(2):103-116.
13. Bora E, Yücel M, Pantelis C. Neurocognitive markers of psychosis in bipolar disorder: a meta-analytic study. *J Affect Disord*. 2010;(Mar):13.
14. Frey BN, Andrezza AC, Nery FG, Martins MR, Quevedo J, Soares JC, Kapczynski F. The role of hippocampus in the pathophysiology of bipolar disorder. *Behav Pharmacol*. 2007;18(5-6):419-430.
15. Hall J, Whalley HC, Marwick K, McKirdy J, Sussmann J, Romaniuk L, Johnstone EC, Wan HL, McIntosh AM, Lawrie SM. Hippocampal function in schizophrenia and bipolar disorder. *Psychol Med*. 2010;40(5):761-770.
16. Benes FM, Kwok EW, Vincent SL, Todtenkopf MS. A reduction of nonpyramidal cells in sector CA2 of schizophrenics and manic depressives. *Biol Psychiatry*. 1998;44(2):88-97.
17. Heckers S, Stone D, Walsh J, Shick J, Koul P, Benes FM. Differential hippocampal expression of glutamic acid decarboxylase 65 and 67 messenger RNA in bipolar disorder and schizophrenia. *Arch Gen Psychiatry*. 2002;59(6):521-529.
18. Konradi C, Eaton M, MacDonald ML, Walsh J, Benes FM, Heckers S. Molecular evidence for mitochondrial dysfunction in bipolar disorder. *Arch Gen Psychiatry*. 2004;61(3):300-308.
19. Knable MB, Barci BM, Webster MJ, Meador-Woodruff J, Torrey EF; Stanley Neuropathology Consortium. Molecular abnormalities of the hippocampus in severe psychiatric illness: postmortem findings from the Stanley Neuropathology Consortium. *Mol Psychiatry*. 2004;9(6):609-620, 544.
20. Benes FM, Lim B, Matzilevich D, Walsh JP, Subburaju S, Minns M. Regulation of the GABA cell phenotype in hippocampus of schizophrenics and bipolars. *Proc Natl Acad Sci U S A*. 2007;104(24):10164-10169.
21. Benes FM, Lim B, Subburaju S. Site-specific regulation of cell cycle and DNA repair in post-mitotic GABA cells in schizophrenic versus bipolars. *Proc Natl Acad Sci U S A*. 2009;106(28):11731-11736.
22. Benes FM. Relationship of GAD(67) regulation to cell cycle and DNA repair in GABA neurons in the adult hippocampus: bipolar disorder versus schizophrenia. *Cell Cycle*. 2010;9(4):625-627.
23. Brambilla P, Perez J, Barale F, Schettini G, Soares JC. GABAergic dysfunction in mood disorders. *Mol Psychiatry*. 2003;8(8):721-737, 715.
24. Benes FM. Amygdalocortical circuitry in schizophrenia: from circuits to molecules. *Neuropsychopharmacology*. 2010;35(1):239-257.
25. Olbrich HG, Braak H. Ratio of pyramidal cells versus non-pyramidal cells in sector CA1 of the human Ammon's horn. *Anat Embryol (Berl)*. 1985;173(1):105-110.
26. Freund TF, Buzsáki G. Interneurons of the hippocampus. *Hippocampus*. 1996;6(4):347-470.
27. Klausberger T, Somogyi P. Neuronal diversity and temporal dynamics: the unity of hippocampal circuit operations. *Science*. 2008;321(5885):53-57.
28. Mann EO, Paulsen O. Role of GABAergic inhibition in hippocampal network oscillations. *Trends Neurosci*. 2007;30(7):343-349.
29. Buzsáki G. *Rhythms of the Brain*. New York, NY: Oxford University Press; 2006.
30. Bonifazi P, Goldin M, Picardo MA, Jorquera I, Cattani A, Bianconi G, Represa A, Ben-Ari Y, Cossart R. GABAergic hub neurons orchestrate synchrony in developing hippocampal networks. *Science*. 2009;326(5958):1419-1424.
31. McBain CJ, Fisahn A. Interneurons unbound. *Nat Rev Neurosci*. 2001;2(1):11-23.
32. Viollet C, Lepousez G, Loudes C, Videau C, Simon A, Epelbaum J. Somatostatinergic systems in brain: networks and functions. *Mol Cell Endocrinol*. 2008;286(1-2):75-87.
33. Binacchi A, Bregola G, Simonato M. On the role of somatostatin in seizure control: clues from the hippocampus. *Rev Neurosci*. 2003;14(3):285-301.
34. Bartos M, Vida I, Jonas P. Synaptic mechanisms of synchronized gamma oscillations in inhibitory interneuron networks. *Nat Rev Neurosci*. 2007;8(1):45-56.
35. Lewis DA, Hashimoto T, Volk DW. Cortical inhibitory neurons and schizophrenia. *Nat Rev Neurosci*. 2005;6(4):312-324.
36. Pantazopoulos H, Lange N, Baldessarini RJ, Berretta S. Parvalbumin neurons in the entorhinal cortex of subjects diagnosed with bipolar disorder or schizophrenia. *Biol Psychiatry*. 2007;61(5):640-652.
37. Dorph-Petersen KA, Nyengaard JR, Gundersen HJ. Tissue shrinkage and unbiased stereological estimation of particle number and size. *J Microsc*. 2001;204(pt 3):232-246.
38. Gundersen HJ. Stereology of arbitrary particles: a review of unbiased number and size estimators and the presentation of some new ones, in memory of William R. Thompson. *J Microsc*. 1986;143(pt 1):3-45.
39. West MJ, Slomianka L, Gundersen HJ. Unbiased stereological estimation of the total number of neurons in the subdivisions of the rat hippocampus using the optical fractionator. *Anat Rec*. 1991;231(4):482-497.
40. Gundersen HJ, Jensen EB. The efficiency of systematic sampling in stereology and its prediction. *J Microsc*. 1987;147(pt 3):229-263.
41. Gundersen HJ. The nucleator. *J Microsc*. 1988;151(pt 1):3-21.
42. Gundersen HJ, Bagger P, Bendtsen TF, Evans SM, Korbo L, Marcussen N, Møller A, Nielsen K, Nyengaard JR, Pakkenberg B, et al. The new stereological tools: disector, fractionator, nucleator and point sampled intercepts and their use in pathological research and diagnosis. *APMIS*. 1988;96(10):857-881.
43. Heckers S. Hippocampus. In: Javitt D, Kantrowitz J, eds. *Handbook of Neurochemistry and Molecular Biology: Schizophrenia*. Vol 315-330. 3rd ed. Berlin, Germany: Springer; 2009.
44. Kempton MJ, Geddes JR, Ettinger U, Williams SC, Grasby PM. Meta-analysis, database, and meta-regression of 98 structural imaging studies in bipolar disorder. *Arch Gen Psychiatry*. 2008;65(9):1017-1032.
45. Arnone D, Cavanagh J, Gerber D, Lawrie SM, Ebmeier KP, McIntosh AM. Magnetic resonance imaging studies in bipolar disorder and schizophrenia: meta-analysis. *Br J Psychiatry*. 2009;195(3):194-201.
46. Amaral D, Lavenex P. Hippocampal neuroanatomy. In: Andersen P, Morris R, Amaral D, Bliss T, O'Keefe J, eds. *The Hippocampus Book*. Oxford, England: Oxford University Press; 2007:37-114.
47. Yushkevich PA, Avants BB, Pluta J, Das S, Minkoff D, Mechanic-Hamilton D, Glynn S, Pickup S, Liu W, Gee JC, Grossman M, Detre JA. A high-resolution computational atlas of the human hippocampus from postmortem magnetic resonance imaging at 9.4 T. *Neuroimage*. 2009;44(2):385-398.
48. Boretius S, Kasper L, Tammer R, Michaelis T, Frahm J. MRI of cellular layers in mouse brain in vivo. *Neuroimage*. 2009;47(4):1252-1260.
49. Ekstrom AD, Bazih AJ, Suthana NA, Al-Hakim R, Ogura K, Zeineh M, Burggren AC, Bookheimer SY. Advances in high-resolution imaging and computational unfolding of the human hippocampus. *Neuroimage*. 2009;47(1):42-49.
50. Hanamiya M, Korogi Y, Kakeda S, Ohnari N, Kamada K, Moriya J, Sato T, Kitajima M, Akamatsu N, Tsuji S. Partial loss of hippocampal striation in medial temporal lobe epilepsy: pilot evaluation with high-spatial-resolution T2-weighted MR imaging at 3.0 T. *Radiology*. 2009;251(3):873-881.
51. Lisman JE. Relating hippocampal circuitry to function: recall of memory sequences by reciprocal dentate-CA3 interactions. *Neuron*. 1999;22(2):233-242.
52. Buzsáki G, Chrobak JJ. Temporal structure in spatially organized neuronal ensembles: a role for interneuronal networks. *Curr Opin Neurobiol*. 1995;5(4):504-510.
53. Buzsáki G. Hippocampal GABAergic interneurons: a physiological perspective. *Neurochem Res*. 2001;26(8-9):899-905.
54. Spencer KM, Nestor PG, Niznikiewicz MA, Salisbury DF, Shenton ME, McCarley RW. Abnormal neural synchrony in schizophrenia. *J Neurosci*. 2003;23(19):7407-7411.
55. Gonzalez-Burgos G, Lewis DA. GABA neurons and the mechanisms of network oscillations: implications for understanding cortical dysfunction in schizophrenia. *Schizophr Bull*. 2008;34(5):944-961.
56. Uhlhaas PJ, Haenschel C, Nikolić D, Singer W. The role of oscillations and synchrony in cortical networks and their putative relevance for the pathophysiology of schizophrenia. *Schizophr Bull*. 2008;34(5):927-943.
57. Sanacora G, Rothman DL, Mason G, Krystal JH. Clinical studies implementing glutamate neurotransmission in mood disorders. *Ann N Y Acad Sci*. 2003;1003:292-308.
58. Frye MA, Tsai GE, Huggins T, Coyle JT, Post RM. Low cerebrospinal fluid glutamate and glycine in refractory affective disorder. *Biol Psychiatry*. 2007;61(2):162-166.
59. Singh V, Muzina DJ, Calabrese JR. Anticonvulsants in bipolar disorder. *Psychiatr Clin North Am*. 2005;28(2):301-323.
60. Clark RE, Squire LR. Classical conditioning and brain systems: the role of awareness. *Science*. 1998;280(5360):77-81.
61. Schacter DL. Memory and awareness. *Science*. 1998;280(5360):59-60.
62. Fanselow MS, Dong HW. Are the dorsal and ventral hippocampus functionally distinct structures? *Neuron*. 2010;65(1):7-19.
63. McClelland JL, McNaughton BL, O'Reilly RC. Why there are complementary learning systems in the hippocampus and neocortex: insights from the successes and

- failures of connectionist models of learning and memory. *Psychol Rev.* 1995; 102(3):419-457.
64. Schacter DL, Addis DR. The cognitive neuroscience of constructive memory: remembering the past and imagining the future. *Philos Trans R Soc Lond B Biol Sci.* 2007;362(1481):773-786.
 65. Wingo AP, Harvey PD, Baldessarini RJ. Neurocognitive impairment in bipolar disorder patients: functional implications. *Bipolar Disord.* 2009;11(2):113-125.
 66. Liu L, Schulz SC, Lee S, Reutiman TJ, Fatemi SH. Hippocampal CA1 pyramidal cell size is reduced in bipolar disorder. *Cell Mol Neurobiol.* 2007;27(3):351-358.
 67. Duan X, Chang JH, Ge S, Faulkner RL, Kim JY, Kitabatake Y, Liu XB, Yang CH, Jordan JD, Ma DK, Liu CY, Ganesan S, Cheng HJ, Ming GL, Lu B, Song H. Disrupted-in-schizophrenia 1 regulates integration of newly generated neurons in the adult brain. *Cell.* 2007;130(6):1146-1158.
 68. Krivosheya D, Tapia L, Levinson JN, Huang K, Kang Y, Hines R, Ting AK, Craig AM, Mei L, Bamji SX, El-Husseini A. ErbB4-neuregulin signaling modulates synapse development and dendritic arborization through distinct mechanisms. *J Biol Chem.* 2008;283(47):32944-32956.
 69. Foland LC, Altshuler LL, Sugar CA, Lee AD, Leow AD, Townsend J, Narr KL, Asuncion DM, Toga AW, Thompson PM. Increased volume of the amygdala and hippocampus in bipolar patients treated with lithium. *Neuroreport.* 2008;19(2):221-224.
 70. Yucel K, McKinnon MC, Taylor VH, Macdonald K, Alda M, Young LT, MacQueen GM. Bilateral hippocampal volume increases after long-term lithium treatment in patients with bipolar disorder: a longitudinal MRI study. *Psychopharmacology (Berl).* 2007;195(3):357-367.
 71. Javadapour A, Malhi GS, Ivanovski B, Chen X, Wen W, Sachdev P. Hippocampal volumes in adults with bipolar disorder. *J Neuropsychiatry Clin Neurosci.* 2010; 22(1):55-62.
 72. Pantazopoulos H, Woo TU, Lim MP, Lange N, Berretta S. Extracellular matrix-glia abnormalities in the amygdala and entorhinal cortex of subjects diagnosed with schizophrenia. *Arch Gen Psychiatry.* 2010;67(2):155-166.
 73. Lavenex P, Lavenex PB, Bennett JL, Amaral DG. Postmortem changes in the neuroanatomical characteristics of the primate brain: hippocampal formation. *J Comp Neurol.* 2009;512(1):27-51.
 74. Chan-Palay V. Somatostatin immunoreactive neurons in the human hippocampus and cortex shown by immunogold/silver intensification on vibratome sections: coexistence with neuropeptide Y neurons, and effects in Alzheimer-type dementia. *J Comp Neurol.* 1987;260(2):201-223.
 75. Schulze TG, Ohlraun S, Czerski PM, Schumacher J, Kassem L, Deschner M, Gross M, Tullius M, Heidmann V, Kovalenko S, Jamra RA, Becker T, Leszczynska-Rodziewicz A, Hauser J, Illig T, Klopp N, Wellek S, Cichon S, Henn FA, McMahon FJ, Maier W, Propping P, Nöthen MM, Rietschel M. Genotype-phenotype studies in bipolar disorder showing association between the DAOA/G30 locus and persecutory delusions: a first step toward a molecular genetic classification of psychiatric phenotypes. *Am J Psychiatry.* 2005;162(11):2101-2108.
 76. Lisman JE, Coyle JT, Green RW, Javitt DC, Benes FM, Heckers S, Grace AA. Circuit-based framework for understanding neurotransmitter and risk gene interactions in schizophrenia. *Trends Neurosci.* 2008;31(5):234-242.
 77. Heckers S. Making progress in schizophrenia research. *Schizophr Bull.* 2008;34(4):591-594.
 78. Rogawski MA, Löscher W. The neurobiology of antiepileptic drugs for the treatment of nonepileptic conditions. *Nat Med.* 2004;10(7):685-692.